FAST INSTABILITY INDICATOR IN FEW DIMENSIONAL DYNAMICAL SYSTEMS.

PIERO CIPRIANI
Istituto Nazionale di Ottica Applicata, L.go E.Fermi, 6 - 50125 - Firenze (Italia)
and
I.C.R.A. - *Coordinating Center - P.le della Repubblica, 10 - 65121 Pescara (Italia)*[*]
E-mail: cipriani@ino.it

MARIA DI BARI
Dip. di Fisica, Univ. di Parma - Parco Area delle Scienze, 7/A - 43100 Parma (Italia)
and
I.N.F.M. - *UdR di Parma*
E-mail: mariateresa.dibari@fis.unipr.it

Using the tools of Differential Geometry, we define a new *fast* chaoticity indicator, able to detect dynamical instability of trajectories much more effectively, (*i.e.*, *quickly*) than the usual tools, like Lyapunov Characteristic Numbers (LCN's) or Poincaré Surface of Section. Moreover, at variance with other *fast* indicators proposed in the Literature, it gives informations about the asymptotic behaviour of trajectories, though being *local* in phase-space. Furthermore, it detects the chaotic or regular nature of geodesics without any reference to a given perturbation and it allows also to discriminate between different regimes (and possibly sources) of chaos in distinct regions of phase-space.

Chaotic dynamics is believed to be the rule rather than the exception in any generic nonlinear dynamical system; however, there is no general *fast* method able to determine what's the fraction of the allowed phase space occupied by chaotic orbits. This problem exists in the case of few degrees of freedom (dof) systems and for many dimensional ones as well, though it originates from different causes in the two situations. Recently the authors derived[4] a *geometric indicator* of Chaos, able to single out the chaotic or regular character of individual orbits simply computing a pair of *short time correlation functions* of geometric quantities defined on the tangent bundle of the system. Here we discuss some points which, in our opinion, make our indicator preferable with respect to other "*fast*" indicators, and, from a practical viewpoint, we compare its *performances* with those of the others, showing the faster convergence properties and the richer amount of information it contains.

In addition to the well known reduction of dynamics to geometry which can be accomplished on the grounds of the Maupertuis principle of Least Action[1], there is a variety of possibilities of transcription of dynamical trajectories into geodesic flows over suitable manifolds. A particularly appealing choice, in the case of generic Lagrangian systems, with a more general than simply quadratic dependence on velocities, is given by the Finsler approach, which furnishes a metric on the tangent bundle of the Lagrangian system under examination[6,7]. Dynamical instability is linked to curvature properties of the manifold through *Jacobi–Levi-Civita* equation for geodesic spread (or a suitable generalization thereof), which describes the evo-

[*]Permanent *postal* address: C.S.S. - via E.Nardi, 14-16 – 02047 – Poggio Mirteto (RI) Italia ; E-mail: cipriani@icra.it

lution of a generic perturbation δq^a to a given geodesic, as a function of the affine parameter, s, along the geodesic itself:

$$\frac{\nabla}{ds}\left(\frac{\nabla \delta q^a}{ds}\right) + \mathcal{H}^a{}_c \delta q^c = 0, \tag{1}$$

where the *stability tensor*[2,3], $\mathcal{H}^a{}_c$, defined along any geodesic, is related to the Finsler curvature tensor, $K^a{}_{bcd}$, associated to the metric, by

$$\mathcal{H}^a{}_c \doteq K^a{}_{bcd} x'^b x'^d \ , \tag{2}$$

and x' is the unit tangent vector to the geodesic. Finsler curvature tensor (and consequently the stability tensor) is a pretty complicated object [6,7]; however the main features of the geodesic flow depend essentially on suitable *averages* and moments of scalars built from $\mathcal{H}^a{}_c$. In the case of N-dof systems, the curvature properties of the associated Finsler manifold are described by the N non trivial *principal sectional curvatures*[3], $\{\lambda_i(s)\}$, which *are specific of each given path*, *i.e.*, depend not only on the point on the configuration space but also on the tangent vector along the given geodesic[a]. If we restrict to two dof systems, the curvature properties of the Finsler manifold are then described by the two principal sectional curvatures $\{\lambda_1, \lambda_2\}$. The *mean* curvature κ and the anisotropy ϑ are defined, in terms of the principal sectional curvatures, simply as

$$\kappa \doteq \frac{\lambda_1 + \lambda_2}{2} \equiv \frac{\mathrm{Tr}(\boldsymbol{\mathcal{H}})}{2} = \frac{\mathsf{Ric}_\mathrm{F}(x')}{2} \quad ; \quad \vartheta \doteq \frac{\lambda_1 - \lambda_2}{2} \ . \tag{3}$$

where it has been exploited the link between the (Finsler generalization of) Ricci curvature along the flow and the trace of the stability tensor. For any realistic dynamical system, it is easy to verify that the associated Finsler manifold and the geodesics on it are characterized by principal sectionals which fluctuate around a well defined average[b], $\lambda_i = \lambda_i(s)$. Schur theorem[10] establishes a link between the anisotropy of a manifold and the fluctuations of the curvatures moving along a given path, in particular along a geodesic, and suggests a possible tool to characterize the interplay between them.

Introducing the correlation function of any two given observables, $X(s) \doteq \tilde{X}[q(s), q'(s)]$ and $Y(s) \doteq \tilde{Y}[q(s), q'(s)]$ computed *over a finite interval*, S, along a geodesic with initial conditions $(\mathbf{q}_0, \mathbf{q}'_0) \equiv [\mathbf{q}(0), \mathbf{q}'(0)]$,

$$\widetilde{\mathcal{C}}_S[X,Y] \ \doteq \ \frac{\langle X \cdot Y \rangle_S}{\left(\langle X^2 \rangle_S \ \cdot \ \langle Y^2 \rangle_S\right)^{1/2}} \ , \tag{4}$$

we define the functional $R_F[S]$ over the given segment of the geodesic, as

$$R_F[S] \ \equiv \ R_F(\mathbf{q}_0, \mathbf{q}'_0) \ \doteq \ \frac{\widetilde{\mathcal{C}}[\vartheta, \delta\vartheta]}{\widetilde{\mathcal{C}}[\kappa, \delta\kappa]} \ \geq \ 0 \ , \tag{5}$$

[a] This is one of the main differences which make the Finsler geometrization more adeherent to the complete dynamics than others, like Jacobi or Eisenhart.

[b] The only requirement is that the phase space is bounded and the dynamical system is singularity-free; though with some cautions the application of our approach can be extended even to singular lagrangians.

where $\delta X(s) \doteq X(s) - \langle X \rangle$. We have shown[4,5] that the stability properties of the geodesic flow, and then the degree of chaoticity of the trajectories, possess an one-to-one correspondence with the value assumed by this functional over any short segment of a geodesic. Just by computing R_F over a few periods along an orbit, suffices to have a reliable indication on its regular or chaotic character. Here we report some supplementary results, still referred to the *paradigmatic* Hénon–Heiles system[9], whose Lagrangian is

$$L(\mathbf{q}, \dot{\mathbf{q}}) = \frac{1}{2}\left(\dot{q}_x^2 + \dot{q}_y^2\right) - \left[\frac{1}{2}\left(x^2 + y^2\right) + x^2 y - \frac{y^3}{3}\right] , \tag{6}$$

which emphasize the much faster convergence of our indicator with respect to the usual ones. A pictorial taste of the reliability and effectiveness of the Finsler indicator, has been given, for example, in figures 1 and 2 of ref.[4], where we made a synoptic comparison of the gray-scale map of R_F with the PSS for a typical energy value ($E = 0.125$), for which the phase space of this system is almost equally populated by chaotic and regular trajectories; noticing that the integration time S, used to produce the map of $R_F[S]$-map is there about two orders of magnitude shorter than the one required to obtain the PSS with a comparable resolution level. Furthermore, we observe that, if a better resolution of the substructures on the surface is sought, the computation of R_F requires obviously only a more careful numerical integration, whereas the PSS needs also to improve the bisection algorithm needed to find the exact intersection point. More detailed results and discussions, and extensive applications to other few dimensional systems can be found elsewhere[5]. To further evaluate quantitatively the fast convergence of the proposed indicator, we report in figure 1 the values of the LCN's and of $R_F[S]$ as a function of *time*[c] for some typical orbits of the same system, which makes self-evident the much faster signature of regular or chaotic motion obtained using the geometric indicator. In addition, we stress also that the values of our indicator are completely independent from any given choice of the initial perturbation vector, whereas this is not true for the computation of the LCN's, whose values, especially for few dof systems, can be strongly influenced by the choice of the orientation of the initial disturbance vector. This is mostly evident if the reference orbit is near the border between regular islands and the stochastic sea, where *stickness* phenomena are expected to occur. The three plots in the figure indeed demonstrate all what has been said here:

- Plot $[A]$, showing the long time behaviour of LCN's, singles out that for some rather *sticky* orbits, the time required for the non vanishing LCN's to converge towards the *true* asymptotic values can be about three orders of magnitude larger than the associated Lyapunov time, $\tau_L \sim LCN^{-1}$.

- Moreover, the two curves labeled as (3) and (3b) show that up to $t \cong 10^3$ the behaviour of two LCN's, computed along the *same orbit* but with a different choice of the orientation of the perturbation vector in phase space, can display completely different behaviours.

[c] See [4,6] for the relationship between the Newtonian time t and the Finsler affine parameter s_F. We recall only that we can always choose, as we did here, $s_F(t) \cong t$.

Figure 1. Convergence properties of LCN's and of the (normalized) geometric indicator R_F: panels [A] and [B] display respectively the long and short time behaviours of LCN's for a set of initial conditions on the energy surface $E = 0.125$. Panel [C] shows the values of R_F for the same trajectories and for two further regular orbits. The much faster convergence of the latter indicator is evident.

- This is confirmed by the behaviour reported in the plot [B], where the same curves of the previous graph are restricted to a relatively short interval, which reveals how, up to $t \sim 200$, LCN's are completely inadequate to discriminate between regular and chaotic orbits.

- Plots in [C] show instead that the (normalized[4]) geometric indicator R_F possess much better convergence properties: it is evident that already at $t \sim 50$ the discrimination between chaotic and regular orbits is clear and the fluctuations around the average for regular orbits are almost negligible. Moreover the values assumed by our indicator give a measure about the *degree of regularity* of non chaotic trajectories, indicating which *topological region* of phase space will become chaotic *earlier*, as we increase the perturbation parameter, *i.e.*, in this case, the energy.

A couple of final comments are in order.

The first one addresses the *dichotomy* encountered in the characterization of dynamical systems, where no intermediate status exist between *ordered* and *chaotic* motions, for a given dynamical system: the picture based on the usual tools shows that the change from asymptotically ordered to chaotic dynamics, presents itself indeed as a *phase transition*, along with a variation of an external parameter (e.g., the energy), with a sudden jump of asymptotic *observables* (e.g., LCN's) from a vanishing value to a finite one. The proposed geometric indicator, though confirming the occurrence of a *change of state* phenomenology, brought to evidence even by local correlation functions, indicates however the presence of gradual, premonitory changes of local observables, accompanying the approach to the *critical point*.

The second remark deals with some recently proposed so-called *fast indicators*, like *rotation angles* and *Fast Lyapunov Indicators*[8,11]. These interesting alternative tools to detect chaoticity, when applied to continuous time dynamical systems, give *"fast"* informations about the *"local"* dynamics; if, inseatd, an asymptotic characterization is sought, then their computation needs, in general, as much as integration time as that required by the evaluation of LCN's. In addition they also make necessarily reference to a given choice of the perturbation vector. Nevertheless they are best suited for the study of the KAM and Nekhoroshev thresholds in the case of discrete time maps, where our approach is instead unsuitable.

In any case, we point out that our *geometric* indicator, which is defined only in terms of the region of the tangent bundle explored by a trajectory, gives a deeper conceptual insight on the sources of Chaos in dynamical systems, just because is strictly linked to the properties of the underlying manifold and make no reference to any perturbations.

References

1. V.I.Arnold *"Mathematical Methods of Classical Mechanics"*, *Springer* (1989).
2. P.Cipriani,*Ph.D. Thesis* - Univ. of Rome - Acad.Year 1992-93 (*in italian*).
3. P.Cipriani, M.Di Bari Plan.Sp.Sci. **46**, 1499 (1998).
4. P.Cipriani, M.Di Bari Phys.Rev.Lett. **81**, 5532 (1998).
5. P.Cipriani, M.Di Bari, submitted to Phys.Rev.E.
6. M.Di Bari, P.Cipriani Plan.Sp.Sci. **46**, 1534 (1998).
7. M.Di Bari *et al.* Phys.Rev.E **55**, 6448 (1997).
8. C.Froeschlé, E.Lega, R.Gonczi Cel.Mech.& Dyn.Astr. **67**, 41 (1997).
9. M.Hénon, C.Heiles Astron.Journ. **69**, 73 (1964).
10. J.L.Synge, A.Schild *"Tensor Calculus"*, *Dover* (1978).
11. N.Voglis, G.Contopoulos, C. Efthymiopoulos Cel.Mech.& Dyn.Astr. **73**, 211 (1999).

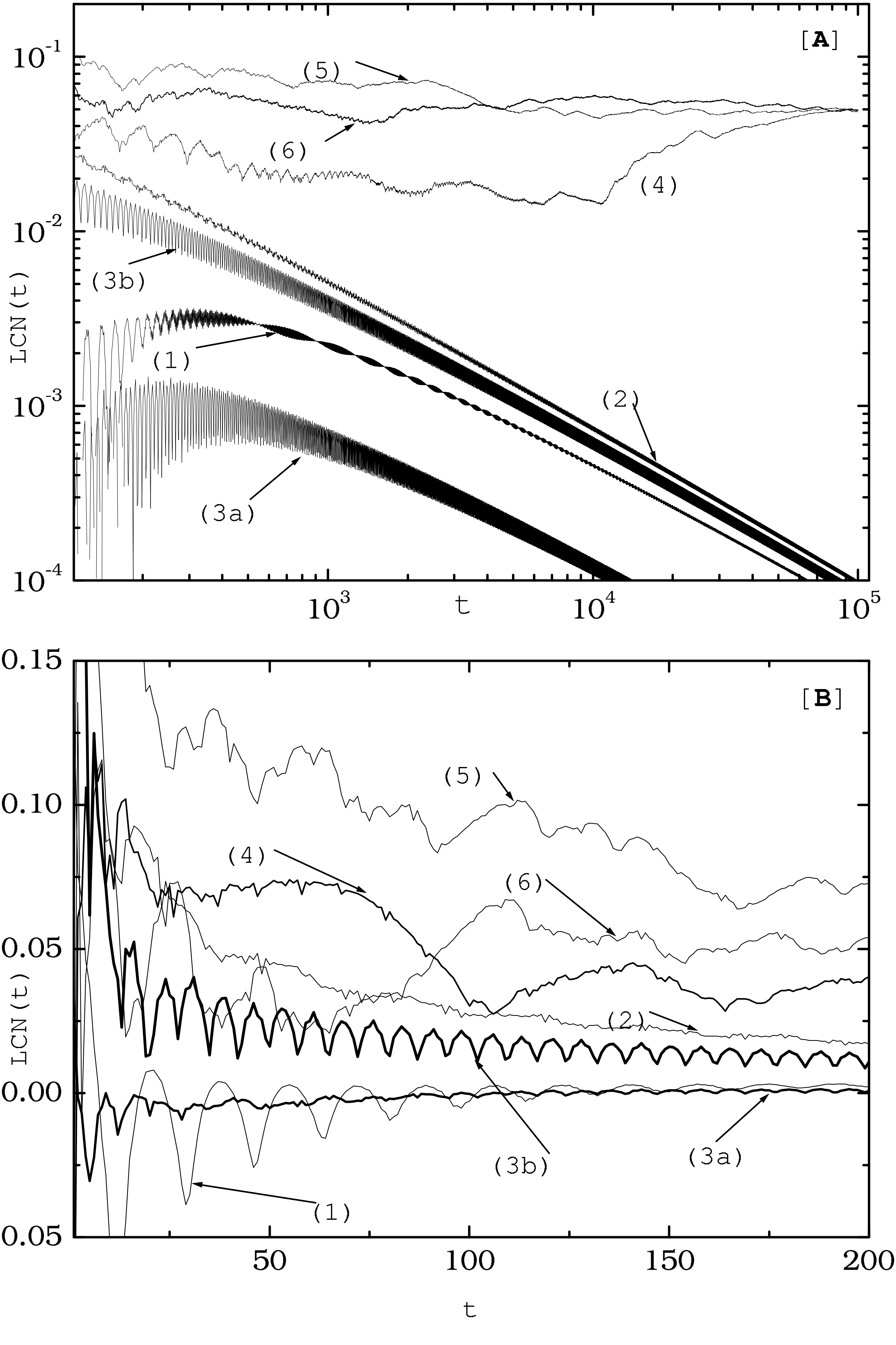
[A]
LCN(t)
t
10^{-1}
10^{-2}
10^{-3}
10^{-4}
10^{3}
10^{4}
10^{5}
(1)
(2)
(3a)
(3b)
(4)
(5)
(6)
[B]
0.15
0.10
0.05
0.00
-0.05
50
100
150
200

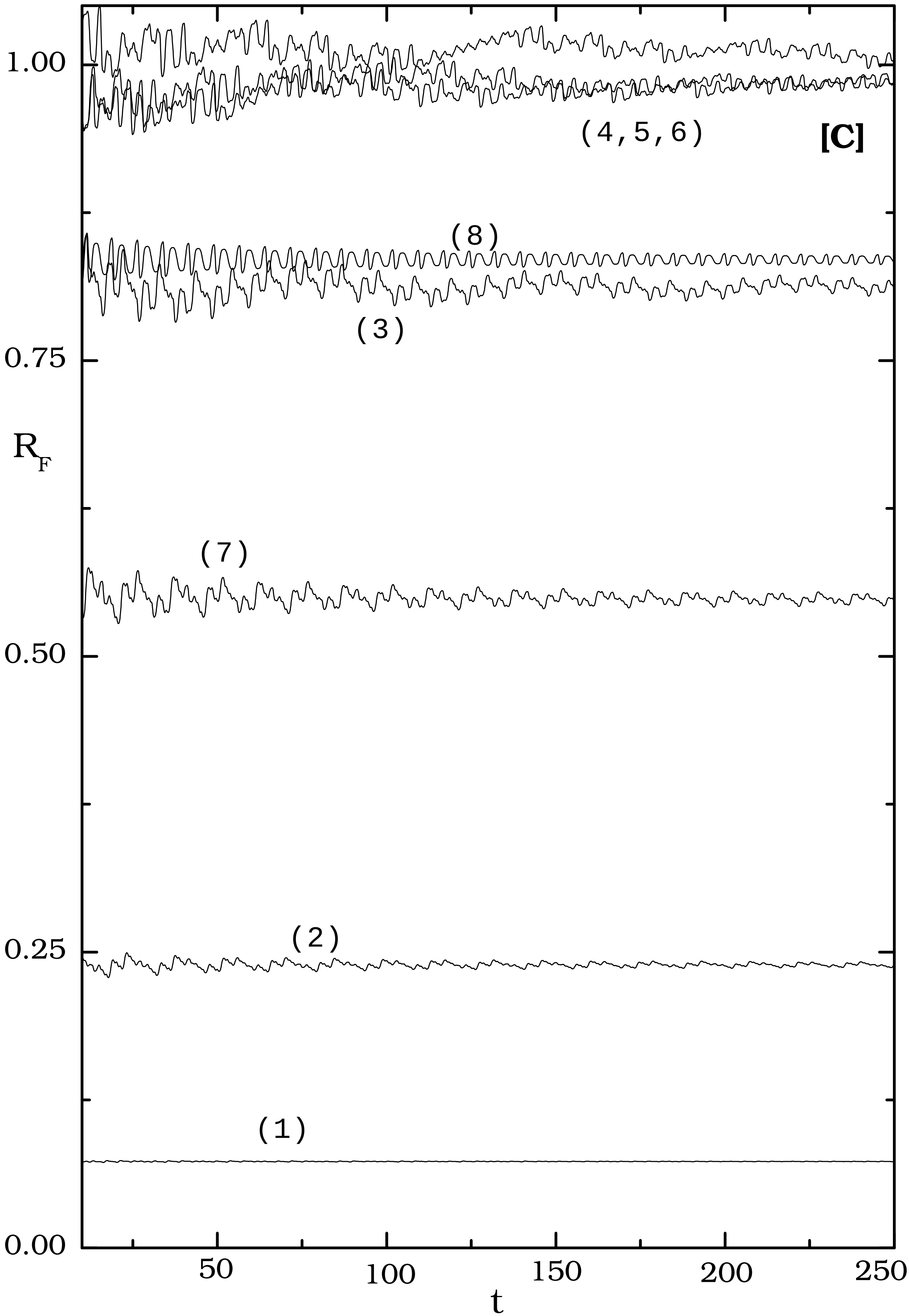

1.00
0.75
0.50
0.25
0.00
R_F
50
100
150
200
250
t
(4,5,6)
[C]
(8)
(3)
(7)
(2)
(1)